A Comparative Study of Harmonic Distortion in Multicarrier Based PWM Switching Techniques for Cascaded H-Bridge Inverters

Pegah HAMEDANI, Abbas SHOULAIE
Electrical Engineering Department, Iran University of Science and Technology, Narmak, Tehran, Iran
p_hamedani@iust.ac.ir

***Abstract*—Multicarrier based PWM switching patterns are commonly utilized to control Cascaded H-bridge (CHB) inverters. The main contribution of this paper is to comprehensively investigate the effect of various multicarrier based PWM techniques on harmonic content of the CHB multilevel inverter. In order to achieve this, both of the CHB output voltage and the input current at power grid side have been taken into account. In this work, various PWM modulations such as level shifted (LS), phase shifted (PS), hybrid, and rotative-LS (R-LS) have been studied through both simulation and implementation of an experimental setup. By extracting the frequency spectrum and calculation of THD and WTHD indices, a quantitative comparative study of various multicarrier PWM techniques has been carried out. According to the results, the R-LS-PWM methods (i.e. R-PD, and two new proposed R-POD and R-APOD) reduce the harmonic distortion of the input current while keeping the obvious advantage of LS-PWM modulation such as lower harmonic distortion of the output voltage. Specially, the proposed R-APOD-PWM modulation offers these preferable privileges at odd frequency ratio values.**

***Index Terms*—converters, harmonic distortion, inverters, modulation, pulse width modulation.**

I. INTRODUCTION

Nowadays, multilevel inverters are widely used because of their superior preferences in power quality improvement [1-6]. Cascaded H-bridge (CHB) Voltage Source Inverter (VSI) is one of the well-known multilevel converter topologies utilized in industrial drive applications. The CHB-VSIs have specific advantages of simplicity, modularity and, less harmonic distortion over other multilevel inverter configurations [1-2].

Various modulation methods have been developed for CHB-VSIs [7-13]. The principal goal is to generate a waveform that best fits a sinusoidal waveform with adjustable amplitude and frequency [14-15].

CHB multilevel VSIs are mainly controlled with multiple carrier-based pulse width modulation (PWM) schemes and can be classified according to the carrier arrangements into various types [14-19]:

- Phase shifted PWM (PS-PWM)
- Level shifted PWM (LS-PWM)
- Hybrid PWM (H-PWM)
- Modified (Rotative) level shifted PWM

Phase shifted PWM method is based on the horizontal phase shift of the triangular carriers [15]. As a result, all the H-bridge cells operate under the same switching frequency. Thus, it results in uniform power distribution between the inverter cells [15]. Furthermore, by using the appropriate angle shift between the windings of the rectifier transformer, some low order input current harmonics can be eliminated [15]. However, since the carrier waveforms are not in phase, some extra dv/dts appear in the output line-to-line voltage that are not generated with level shifted methods [15]. This results in a higher output voltage distortion [15].

LS-PWM method can be categorized into different kinds [16-17]:

- Phase Disposition (PD-PWM).
- Phase Opposition Disposition (POD-PWM)
- Alternative Phase Opposition Disposition (APOD-PWM)

In the level shifted PWM methods the carriers are arranged with vertical amplitude displacements [14-16]. The problem with LS-PWM method is that uneven power will be distributed between the inverter cells and the diode rectifiers. Hence, input current harmonics are not canceled, despite multi-pulse configuration and winding angle shifts [15].

In order to combine the benefits of PS-PWM and LS-PWM switching schemes, Hybrid PWM (H-PWM) techniques have been developed [18-19].

Furthermore, in [15] the idea of a rotative PD-PWM (R-PD-PWM) technique has been proposed that modifies the switching pattern of the PD-PWM modulation method in order to achieve uniform power distribution between the inverter cells and the diode rectifiers. This will result in good quality output voltage and harmonic cancellation of input current [15]. This modulation strategy has been implemented only on the PD-PWM method and only through simulation. In this paper, the suggested modulation technique of [15] has been applied for modification of other LS-PWM methods including POD and APOD-PWM through both simulation and experimental implementation.

Although many investigations have been performed until now, the lack of a comprehensive comparison of all the modulation schemes is necessarily required. Consequently, the main objective of this paper is to study the effect of all mentioned PWM switching techniques on the harmonic distortion of five-level CHB-VSI. Unlike lots of previously published investigations, which only consider the output voltage quality, in this work both the input current at power grid side and the CHB output voltage, have been investigated. The study has been conducted through both simulations and experiments.

Digital Object Identifier 10.4316/AECE.2016.03003

II. Topology Description of the H-Bridge Multilevel Inverter

The graphical representation of the five-level CHB-VSI is represented in Fig. 1. The switches S_{11}, S_{12},…, S_{22} represent IGBTs with back-to-back diodes [20]. The dc sources are usually obtained by multi-pulse diode rectifiers or batteries [20]. Multi-pulse diode rectifiers normally consist of three-phase full bridge diode rectifiers, capacitive dc-links and input transformers with proper angle shift between the windings [15]. In this way, the harmonic content of the input current will be reduced. The angle shift depends on the number of inverter cells. In Fig. 2, the appropriate power circuit configuration for five-level CHB-VSI is illustrated.

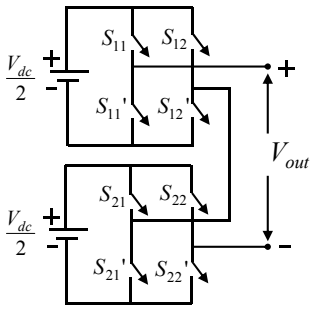

Figure 1. Five-level CHB-VSI configuration

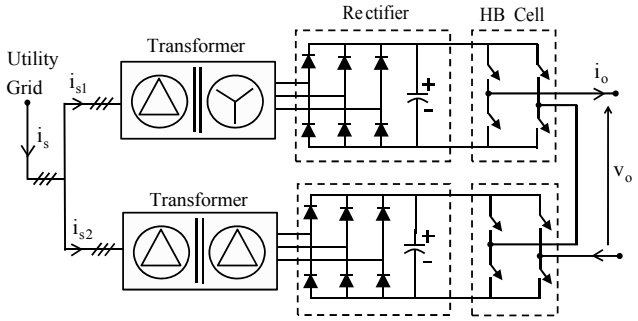

Figure 2. 12-pulse diode rectifier for five-level CHB-VSI

III. Multicarrier Based PWM Switching Methods for the CHB-VSI

A. LS-PWM Switching Methods

For an *m*-level inverter, *m-1* triangular carriers with equal frequencies f_s and amplitudes A_c are vertically and continuously arranged [16-17]. The sinusoidal modulating signal has amplitude A_m, the frequency f_m, and no dc offset [16-17]. The amplitude modulation term m_a and the frequency modulation term m_f can be described as [16-17]:

$$m_a = \frac{A_m}{(m-1)A_c} \tag{1}$$

$$m_f = \frac{f_s}{f_m} \tag{2}$$

It should be noted that in the present work, the angle displacement between the reference signal and the first positive carrier signal is considered constant and equal to zero ($\varphi = \circ$). The modulating signal is steadily compared with the triangular carriers to produce the switching pulses [16-17]. Fig. 3 illustrates the PD-PWM scheme, the generated switching signals (according to Fig. 1), the output voltages of the HB cells, and the total CHB output voltage. Note that the carrier signals are demonstrated in this figure with lower frequency than in practice, only to show the commutation pattern more clearly. As it is clear from Fig. 3 (a), in PD-PWM method all the carriers have the same phase. Fig. 4 (a) shows the POD-PWM in which all the positive carriers are in phase, but with a phase shift of 180º regarding to the negative carriers [16]. As depicted in Fig. 4 (b), in the APOD-PWM each carrier has a phase shift of 180º from the adjacent carriers [16].

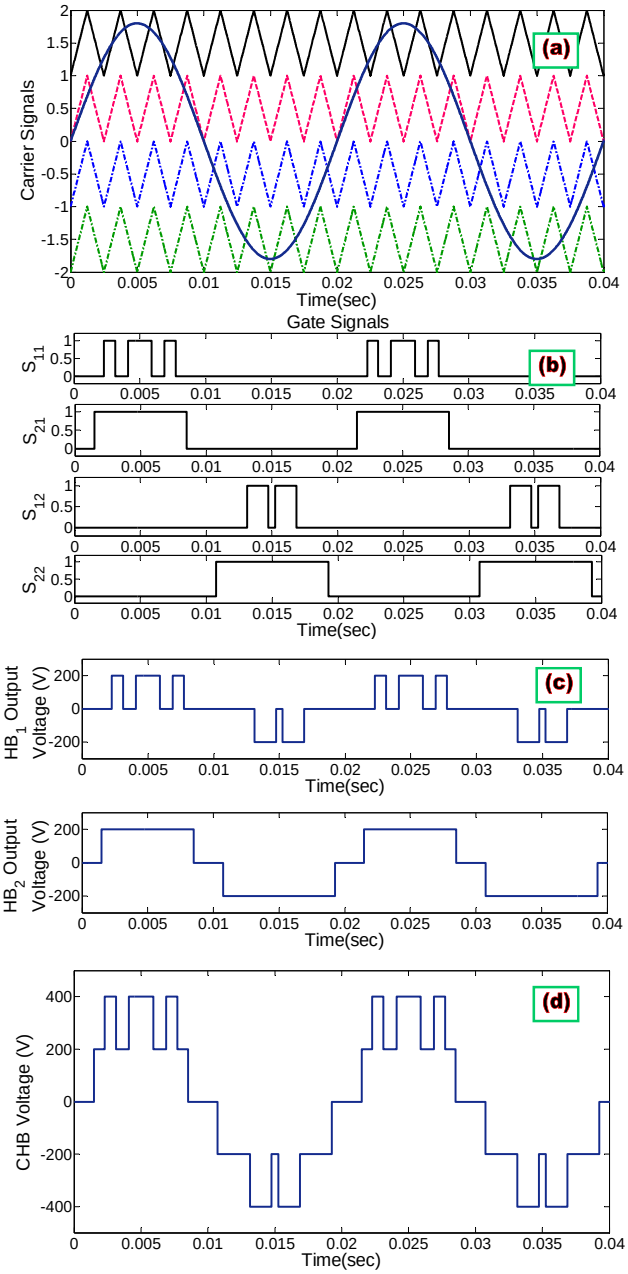

Figure 3. PD-PWM methods: a) modulation scheme, b) gate signals, c) HB cells output voltage, d) CHB output voltage

B. PS-PWM Switching Methods

In the PS-PWM method, for an *m*-level inverter, *m-1* triangular carriers with equal frequencies f_s and amplitudes A_c are utilized which are phase shifted by $\varphi_{cr} = 360^\circ/(m-1)$ to each other [16-17]. The sinusoidal modulating signal has amplitude A_m, the frequency f_m, and no dc offset. The main advantage of this modulation strategy is the uniform power distribution between the inverter cells [16-17]. The amplitude modulation term m_a and the frequency modulation term m_f can be expressed as [16-17]:

$$m_a = \frac{A_m}{A_c} \tag{3}$$

$$m_f = \frac{f_s}{f_m} \tag{4}$$

Fig. 5 illustrates the carrier and reference signal waveforms of the PS-PWM switching scheme. Like all other PWM switching techniques in this work, the reference waveform is continuously compared with the carrier signals. If the reference is greater than each carrier signal, then the corresponding switching device will be turned on.

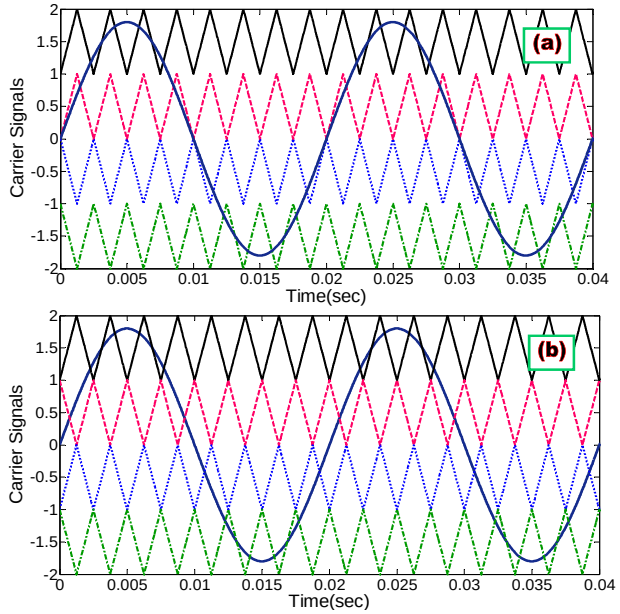

Figure 4. Level shifted PWM methods: a) POD-PWM, b) APOD-PWM

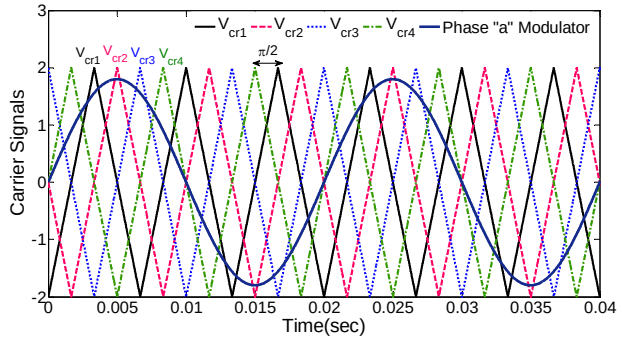

Figure 5. Phase shifted PWM (PS-PWM) switching scheme

C. Hybrid PWM Switching Methods

The hybrid modulation strategies combine the features of LS-PWM and PS-PWM methods [18-19]. Two general hybrid multicarrier PWM switching techniques are investigated in this work for five-level CHB-VSI.

1) H1-PWM:

In this modulation scheme, first, each carrier signal is cut into $2N$ parts with equal heights, and then a phase shift by $\pi/2N$ radian is applied to these parts to become in phase with respect to each other [18-19]. The result is a set of waveforms which is compared with the sinusoidal modulating waveform to generate the gate signal of switch S_{11} (Fig. 6 (a)). The gate signals of the remaining switches will be produced by shifting these set of carriers for switch S_{11} by $\pi/2N$ radian. Fig. 6 shows the sets of carrier signals, the gate signals, and the total CHB output voltage.

For an m-level inverter, the amplitude modulation term m_a and the frequency modulation term m_f can be described as:

$$m_a = \frac{A_m}{(m-1)A_c} \tag{5}$$

$$m_f = \frac{f_s}{f_m} \tag{6}$$

where A_m and f_m are the amplitude and frequency of the modulating signal, respectively. A_c and f_s are the amplitude and frequency of the carrier signal, respectively.

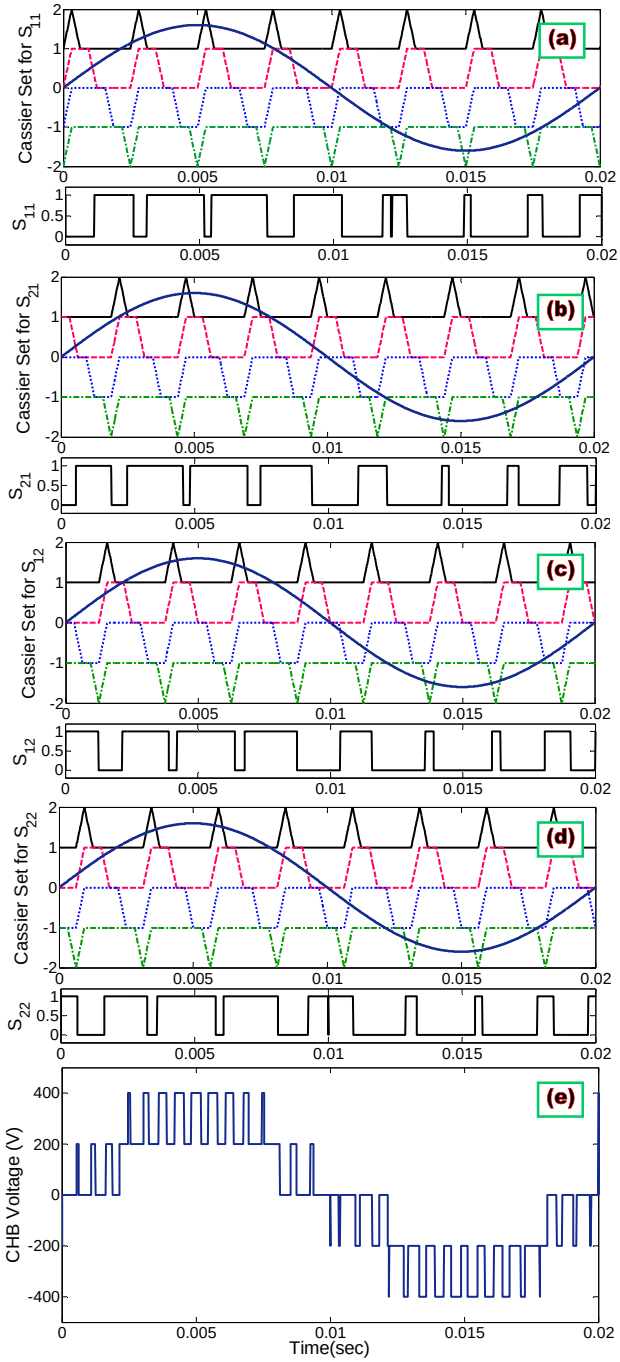

Figure 6. H1-PWM method: a) set of carriers, reference and gate signals of switch S_{11}, b) set of carriers, reference and gate signals of switch S_{21}, c) set of carriers, reference and gate signals of switch S_{12}, d) set of carriers, reference and gate signals of switch S_{22}, e) CHB output voltage

2) H2-PWM:

In this modulation scheme, two carrier signals control the

left and right arms in each HB cell of the inverter [19]. These two carrier signals are located symmetrically above and below the horizontal axis and have equal amplitudes, phases, and frequencies and. After phase shifting of these two signals by $2\pi/N$ radian, the other $2N-2$ carrier signals will be generated which control the remaining HB cells. Fig. 7 represents the carrier and modulating signal waveforms of the H2-PWM scheme.

For an m-level inverter, the amplitude modulation term m_a and the frequency modulation term m_f can be expressed as:

$$m_a = \frac{2A_m}{(m-1)A_c} \tag{7}$$

$$m_f = \frac{f_s}{f_m} \tag{8}$$

where A_m and f_m are the amplitude and frequency of the modulating signal, respectively. A_c and f_s are the amplitude and frequency of the carrier signal, respectively.

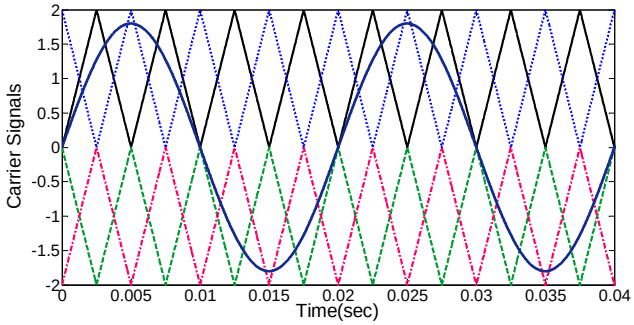

Figure 7. H2-PWM switching scheme

D. Rotative PWM Switching Methods

As mentioned before, PS-PWM method leads to an even power distribution between the inverter cells, which in turn results in harmonic cancelations of the input current at grid side [15]. On the other hand, LS-PWM methods lead to higher output voltage quality and less harmonic distortion in the output voltage waveform. The method proposed in [15], presents a modified PD-PWM method that rotates the carrier signals between different level shifts at every modulation cycle. The level rotations are performed separately between positive and negative carriers [15]. The rotation of the carrier signals is performed by addition of a square waveform with half the frequency of the carriers [15]. Thus, the rotative switching pattern results in uniform power distribution among the inverter cells.

As already mentioned, the R-PD-PWM has been proposed in [15]. In this paper, the modification pattern of [15] has been successfully applied on other LS-PWM switching techniques like POD-PWM and APOD-PWM methods. In Fig. 8 (a)-(c) the carrier and reference signal waveforms of R-PD-PWM, R-POD-PWM and R-APOD-PWM methods are shown, respectively.

Note that in case of R-PD-PWM and R-POD-PWM, the CHB output voltage waveform is similar to the traditional PD-PWM and POD-PWM, respectively. Therefore, the CHB voltage waveforms, the harmonic spectrums, and the THD index values for both methods are almost similar. However, the CHB output voltage waveforms of the traditional APOD-PWM and the R-APOD-PWM are different.

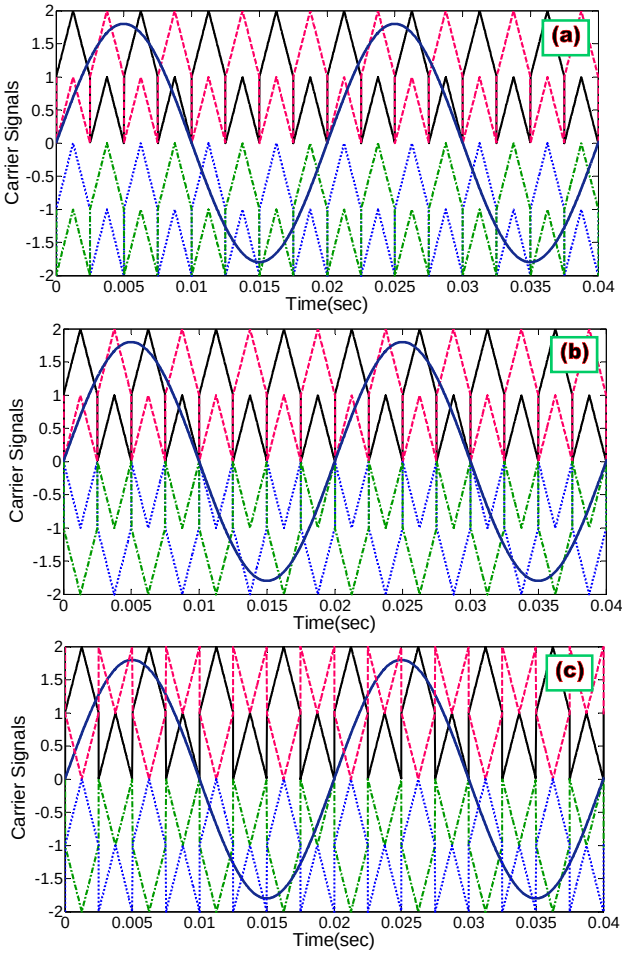

Figure 8. R-LS-PWM methods: a) R-PD-PWM, b) R-POD-PWM, c) R-APOD-PWM

IV. Results and Discussions

A. Effect of Symmetry

In this section, the symmetry of the five-level CHB output voltage waveforms, which affect the harmonic content of the spectrum, has been studied for both even and odd m_f values. The HB cells are supplied through 200 V dc voltage sources. In Fig. 9 to Fig. 15 the output voltage waveforms of various PWM methods have been depicted for even and odd m_f values, m_a=0.9, and f_m=50 Hz.

As shown in the figures, the PD-PWM (traditional or rotative) method leads to odd symmetry for even m_f values (m_f=4). Therefore, in the harmonic spectrum both even and odd harmonic orders will appear. On the other hand, for odd m_f values (m_f=5), the PD-PWM method leads to half wave symmetry and thus, in the harmonic spectrum only odd harmonic orders will exist.

The output voltage waveforms of the POD-PWM (traditional or rotative) and the traditional APOD-PWM methods have quarter waveform symmetry for even m_f values (m_f=4). Therefore, in the corresponding spectrums, the main harmonic orders occur in the sidebands around the carrier frequency and no harmonics will appear at multiples of f_c.

The output voltage waveforms of the POD-PWM (traditional or rotative) and the traditional APOD-PWM methods for odd m_f values (m_f=5) yield only odd symmetry and thus, both even and odd harmonic orders will appear in the spectrum.

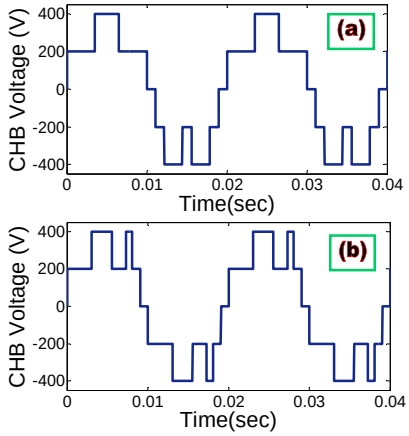

Figure 9. The CHB output voltage with PD-PWM for a) even m_f (m_f=4), b) odd m_f (m_f=5)

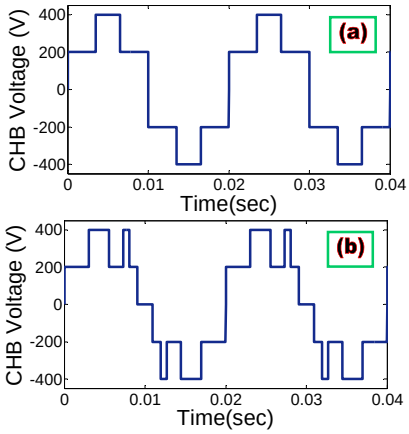

Figure 10. The CHB output voltage with POD-PWM for a) even m_f (m_f=4), b) odd m_f (m_f=5)

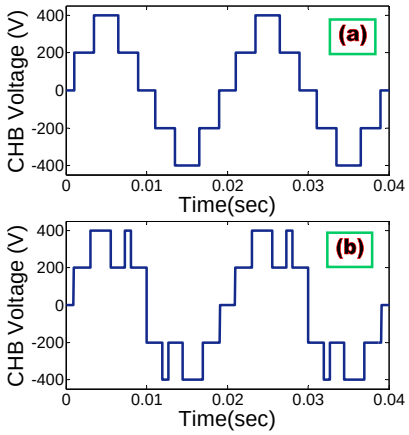

Figure 11. The CHB output voltage with APOD-PWM for a) even m_f (m_f=4), b) odd m_f (m_f=5)

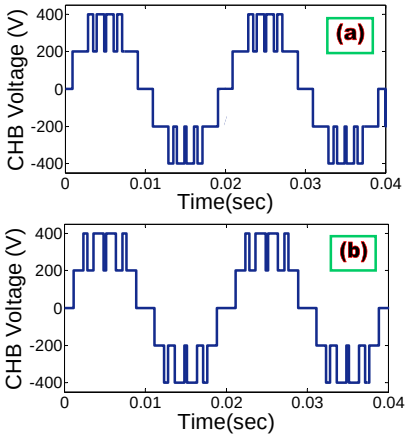

Figure 12. The CHB output voltage with PS-PWM for a) even m_f (m_f=4), b) odd m_f (m_f=3)

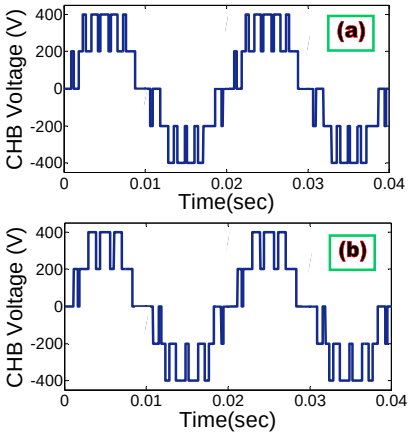

Figure 13. The CHB output voltage with H1-PWM for a) even m_f (m_f=4), b) odd m_f (m_f=3)

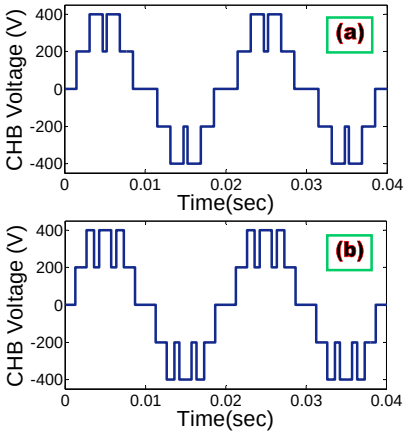

Figure 14. The CHB output voltage with H2-PWM for a) even m_f (m_f=4), b) odd m_f (m_f=5)

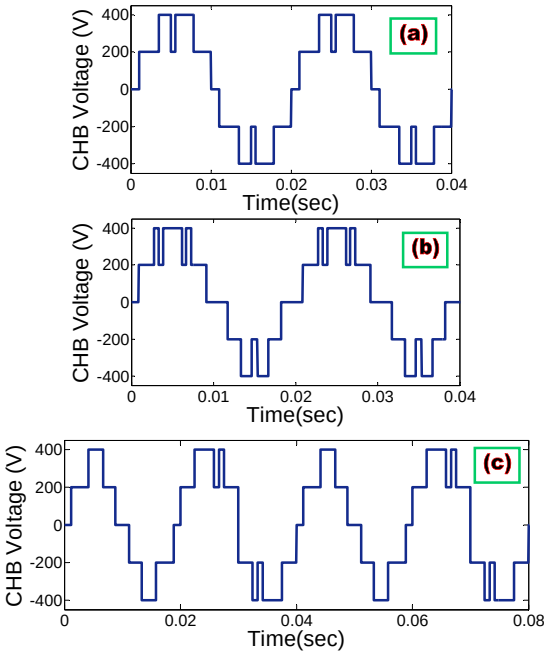

Figure 15. The CHB output voltage with R-APOD-PWM for a) even and multiple of four m_f (m_f=4), b) even but not multiple of four m_f (m_f=6), c) odd m_f (m_f=3)

The output voltage waveforms of both PS-PWM and H2-PWM methods have quarter waveform symmetry for both even and odd m_f values (i.e. m_f=4, m_f=3 for PS and m_f=4, m_f=5 for H2). Accordingly, for even m_f values, the main harmonic orders occur in the sidebands around the carrier frequency and no harmonics will appear at multiples

of f_c in the spectrums. However, for odd m_f values, the odd multiples of f_c are located in the spectrum whereas the even multiples of f_c do not appear in the spectrum.

The H1-PWM method only leads to odd symmetry in the voltage waveform for both even and odd m_f values (m_f=4 and m_f=3). Thus, both even and odd harmonic orders exist in the harmonic spectrum.

The output voltage waveform of the R-APOD-PWM switching scheme has half wave symmetry when m_f is even and multiple of four (like m_f=4). When m_f is even but not multiple of four (like m_f=6), the voltage waveforms has only odd symmetry. On the other hand, for odd m_f values (m_f=5), the R-APOD-PWM modulation leads to an odd waveform that is made up of two different odd waveforms which alternate one after the other.

B. Harmonic Analysis of the CHB Output Voltage

In the next step, the influence of various PWM switching techniques on harmonic distortion of the CHB output voltage has been investigated. The HB cells are supplied through 200 V dc supplies. In Fig. 16 to Fig. 22 the frequency spectrums of the CHB output voltage waveforms for different PWM methods have been plotted. The frequencies of the reference and the carrier signals are considered 50 Hz and 2 KHz (m_f=40), respectively. The amplitude modulation term is considered m_a=0.9.

As shown in the figures, the harmonic content of the voltage waveforms is in accordance with the waveform symmetry discussed before. In the frequency spectrums of PD-PWM, POD-PWM, APOD-PWM, R-PD-PWM, and R-POD-PWM switching patterns, the harmonic cancellation up to the carrier frequency f_c (2 KHz) or its sidebands is obtained. In other word, the principal harmonic orders are located at m_f=40 order or its sidebands. The significant harmonics in the spectrum of the R-APOD-PWM method appear in $f_c/2$, $3f_c/2$, $2f_c$,… . Nevertheless, in the carrier frequency f_c (2 KHz) and its sidebands, the harmonic orders do not appear. For PS-PWM and H1-PWM methods, the harmonic cancellation up to $4f_c$ and its sidebands in the voltage waveform is achieved, whereas H2-PWM method results in the harmonic cancellation up to $2f_c$ and its sidebands in the inverter voltage output.

In addition, in order to have a comprehensive comparison between various multi-carrier PWM techniques, the Total Harmonic Distortion (THD) and Weighted Total Harmonic Distortion (WTHD) indices of the five-level CHB output voltages have been computed and demonstrated in Fig. 23 to Fig. 26 for m_f=40,41 and m_a=0.6,0.75,0.9. Note that for a voltage signal, the THD and WTHD can be defined as:

$$THD = \frac{\sqrt{\sum_{h=2}^{h_{\max}} V_h^{\,2}}}{V_1} \tag{9}$$

$$WTHD = \frac{\sqrt{\sum_{h=2}^{h_{\max}} (V_h / h)^2}}{V_1} \tag{10}$$

where V_h is the rms value of harmonic order h. For a current signal, the THD and WTHD can be written in the same way.

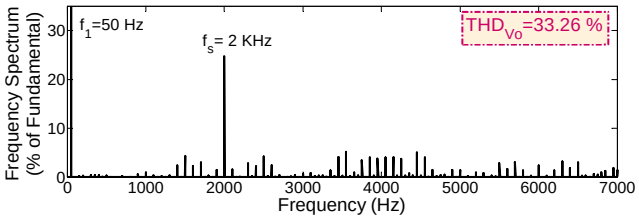

Figure 16. Frequency spectrum of the CHB output voltage with PD-PWM or R-PD-PWM (f_m=50Hz, m_f=40, m_a=0.9)

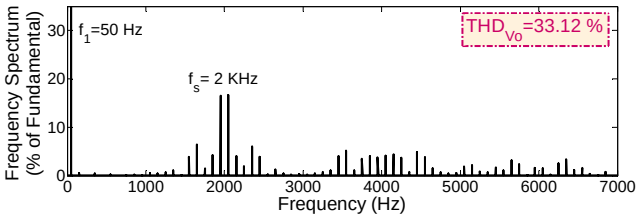

Figure 17. Frequency spectrum of the CHB output voltage with POD-PWM or R-POD-PWM (f_m=50Hz, m_f=40, m_a=0.9)

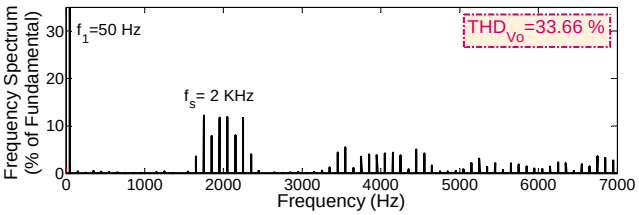

Figure 18. Frequency spectrum of the CHB output voltage with APOD-PWM (f_m=50Hz, m_f=40, m_a=0.9)

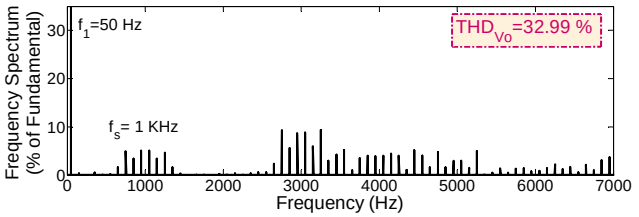

Figure 19. Frequency spectrum of the CHB output voltage with R-APOD-PWM (f_m=50Hz, m_f=40, m_a=0.9)

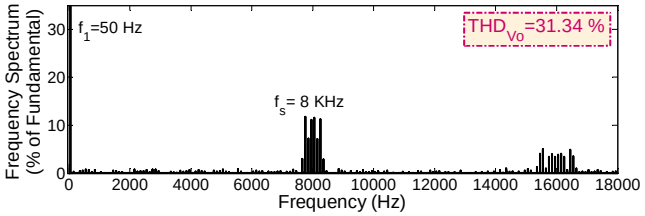

Figure 20. Frequency spectrum of the CHB output voltage with PS-PWM (f_m=50Hz, m_f=40, m_a=0.9)

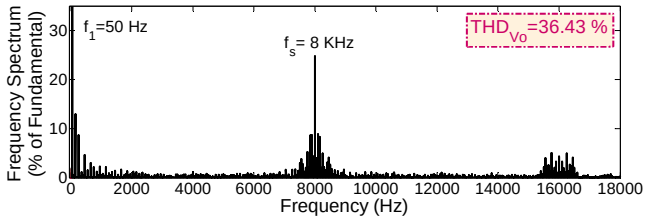

Figure 21. Frequency spectrum of the CHB output voltage with H1-PWM (f_m=50Hz, m_f=40, m_a=0.9)

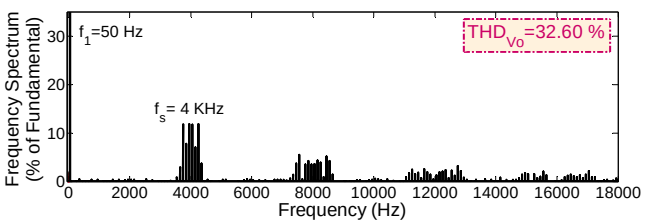

Figure 22. Frequency spectrum of the CHB output voltage with H2-PWM (f_m=50Hz, m_f=40, m_a=0.9)

It is clear from the results that for the odd m_f value (m_f=41), the minimum THD indices of CHB voltages belong to the R-APOD-PWM method. Furthermore, for the odd m_f value, the minimum WTHD indices of CHB voltages are related to the PS-PWM and H2-PWM switching patterns. This means that even though the harmonic components of these two methods have higher amplitudes, their harmonic orders are shifted to higher frequencies in comparison with other PWM methods.

In case of the even m_f value (m_f=40), the lowest THD and WTHD values belong to PS-PWM method, which are due to the lower harmonic amplitudes and higher harmonic frequencies, respectively. Nevertheless, the PS-PWM technique leads to extra dv/dts in the output line-to-line voltages especially at low amplitude modulation term (m_a) values [15].

The PS-PWM, H1-PWM, and H2-PWM in comparison with LS-PWM methods result in higher carrier frequencies (f_c).

Consequently, the traditional and rotative LS-PWM methods in comparison with other PWM switching techniques, offer high quality CHB output voltages. Specially, the proposed R-APOD-PWM method achieves the lowest voltage distortion at odd frequency term (m_f) values.

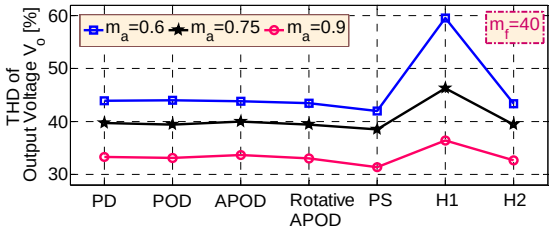

Figure 23. THD values of the CHB output voltage with different PWM methods for even m_f (m_f=40)

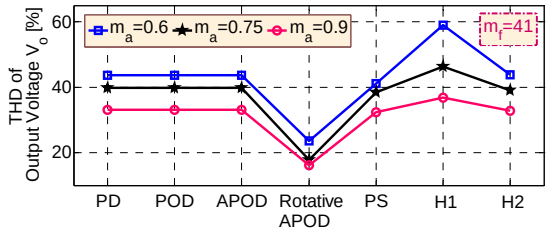

Figure 24. THD values of the CHB output voltage with different PWM methods for odd m_f (m_f=41)

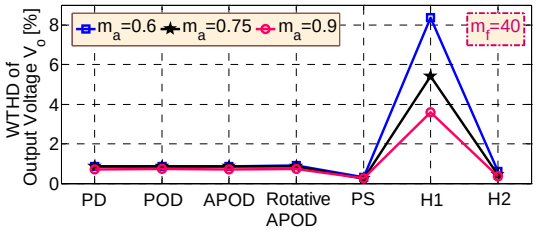

Figure 25. WTHD values of the CHB output voltage with different PWM methods for even m_f (m_f=40)

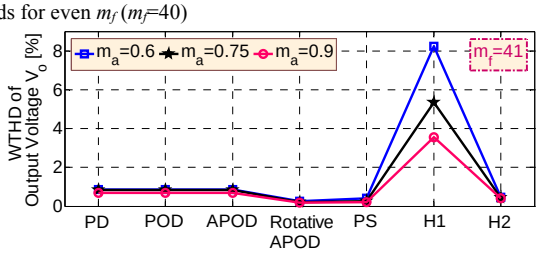

Figure 26. WTHD values of the CHB output voltage with different PWM methods for odd m_f (m_f=41)

C. Harmonic Analysis of the CHB Input Current

In this section, the effect of different PWM switching techniques on harmonic contents of the input current in a five-level CHB-VSI has been investigated. In order to achieve this, the CHB-VSI is supplied with 12-pulse diode rectifiers according to Fig. 2. The 12-pulse diode rectifiers are composed of two three-phase full bridge diode rectifiers, two capacitive dc-links, a Δ/Y transformer, and a Δ/Δ transformer. Simulation of the proposed CHB-VSI supplied with 12-pulse diode rectifier has been implemented using MATLAB/Simulink software. The inverter is loaded by a resistive-inductive load. The main parameters are given in the Appendix A.

Fig. 27 and Fig. 28 depict the CHB output current, CHB output voltage and its frequency spectrum, primary currents of Δ/Y and Δ/Δ transformers, and the input current and its frequency spectrum for traditional PD-PWM and R-PD-PWM, respectively (with f_1=50 Hz, m_a=0.65, and m_f=40). As expected, due to the unbalanced power distribution between the HB cells of the CHB-VSI in PD-PWM strategy, the 5th and 7th harmonic orders will appear in the frequency spectrum of input current. However, for the R-PD-PWM strategy, the 5th and 7th harmonic orders do not exist in the frequency spectrum of input current.

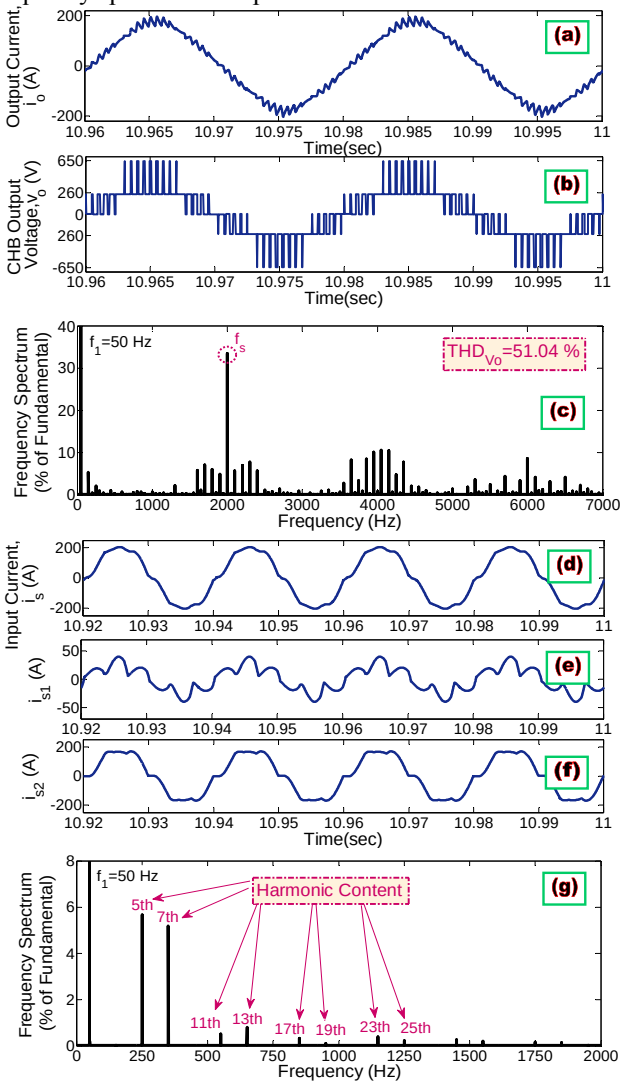

Figure 27. PD-PWM method: a) load current, b) CHB output voltage, c) frequency spectrum of CHB output voltage, d) primary current of Δ/Y transformer, e) primary current of Δ/Δ transformer, f) power grid current, and g) Frequency spectrum of power grid current

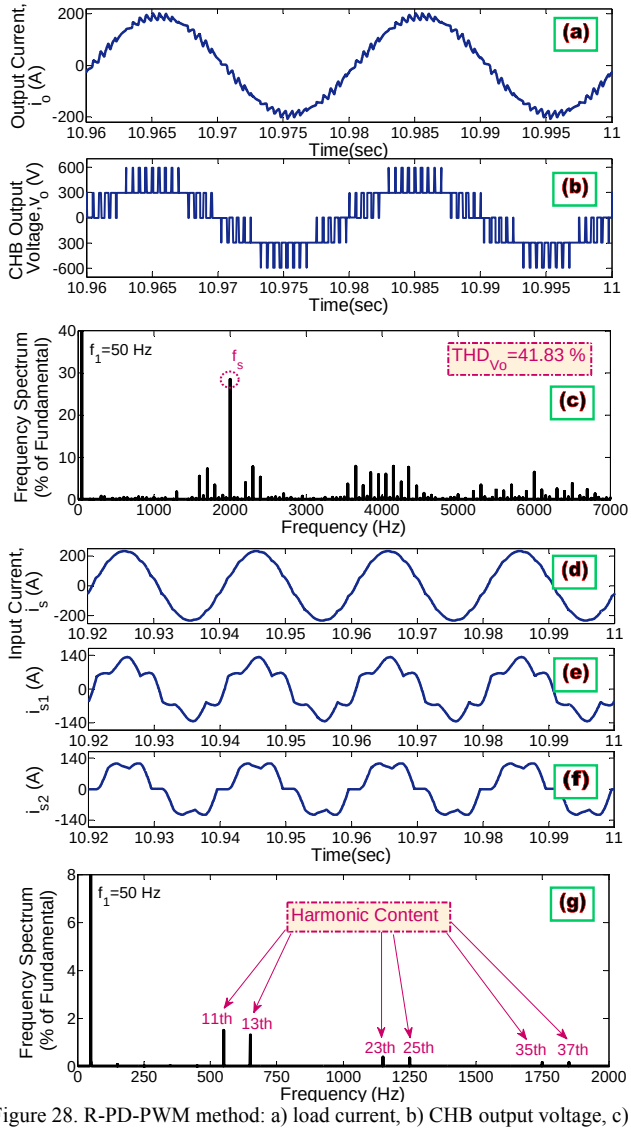

Figure 28. R-PD-PWM method: a) load current, b) CHB output voltage, c) frequency spectrum of CHB output voltage, d) primary current of Δ/Y transformer, e) primary current of Δ/Δ transformer, f) power grid current, and g) frequency spectrum of power grid current

It should be noted that due to the unbalanced power distribution and different loading conditions of the inverter cells, the power which flows through the HB cells, rectifiers, and phase-shift transformers will be different in case of traditional LS-PWM methods. Therefore, even though the nominal line voltages of the Δ/Y and Δ/Δ transformers are considered equal, the line voltages and thus, the rectified dc voltages become unequal. Consequently, the harmonic contents of the CHB output voltage will increase. This is shown in Fig. 27 (b) and Fig. 28 (b).

Furthermore, in order to have a comprehensive comparison between various multi-carrier PWM techniques, the THD and WTHD values of the CHB-VSI input current waveforms at ac grid side have been calculated and demonstrated in Fig. 29 to Fig. 32 for m_f=40,41 and m_a=0.6,0.75,0.9 and with three load types (i.e. R-L, R-L-C, R-C). The load parameters are given in the Appendix A.

In Table I, the effect of various multi-carrier PWM techniques on harmonic contents of the input current waveform at ac grid side have been illustrated. It is clear from the results that in the R-LS-PWM (i.e. R-PD, R-POD, and R-APOD), PS-PWM, and H2-PWM switching techniques, the 5th and 7th harmonic orders will not appear in the frequency spectrum of input current and therefore, the harmonic distortion will be reduced in comparison with other modulation schemes.

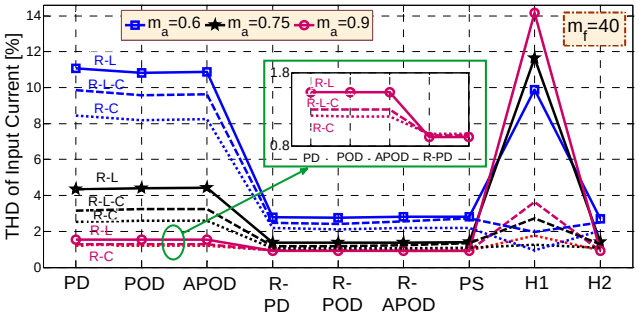

Figure 29. THD values of the CHB input current with different PWM methods for even m_f (m_f=40)

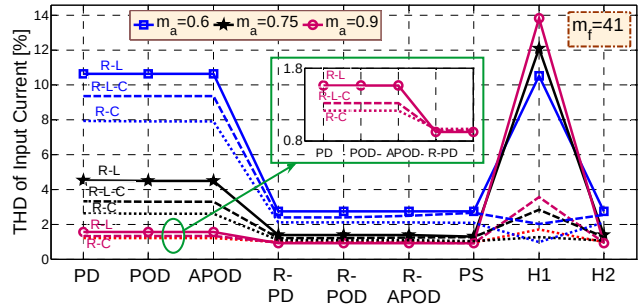

Figure 30. THD values of the CHB input current with different PWM methods for odd m_f (m_f=41)

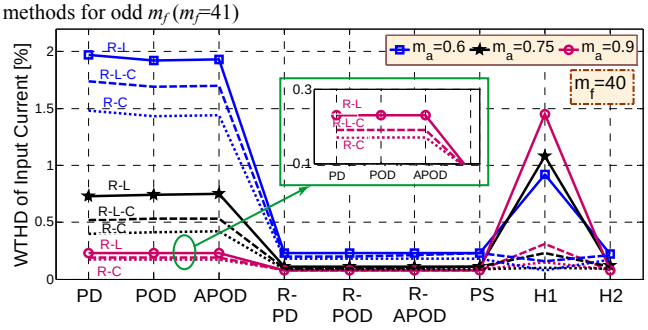

Figure 31. WTHD values of the CHB input current with different PWM methods for even m_f (m_f=40)

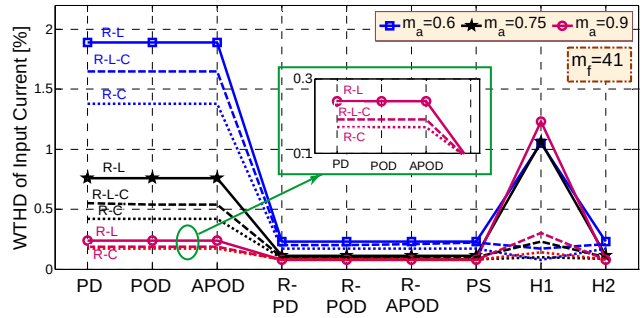

Figure 32. WTHD values of the CHB input current with different PWM methods for odd m_f (m_f=41)

TABLE I. HARMONIC ORDERS OF THE INPUT CURRENT FOR DIFFERENT PWM SCHEMES

		Harmonic order					
		5th	7th	11th	13th	17th	19th
PWM Modulations	PD	√	√	negligible	√	√	√
	POD	√	√	negligible	√	√	√
	APOD	√	√	negligible	√	√	√
	R-PD	-	-	√	√	-	-
	R-POD	-	-	√	√	-	-
	R-APOD	-	-	√	√	-	-
	PS	-	-	√	√	-	-
	H1	√	√	√	√	√	√
	H2	-	-	√	√	-	-

It is clear from the results that the R-LS-PWM (i.e. R-PD,

R-POD, and R-APOD), PS-PWM, and H2-PWM techniques reduce the harmonic contents of the input current. This is due to the uniform power distribution of the HB cells which results in harmonic cancellation of the input current. Nevertheless, as previously mentioned, PS-PWM and H2-PWM methods result in higher distortion of the output line-to-line voltages when compared with R-LS-PWM schemes especially at low amplitude modulation term (m_a) values.

Consequently, the R-LS-PWM methods in comparison with all other PWM modulations, offer relatively higher quality input currents at power grid side as well as lower harmonic distortion in the CHB output voltages. In other words, the R-LS-PWM methods join the privileges of both PS-PWM and the traditional LS-PWM modulations.

V. Experimental Results

In order to confirm the theoretical results, a five-level CHB-VSI prototype has been constructed using eight BUP314D 1200V/42A IGBTs with back-to-back diodes. The CHB-VSI is supplied through two isolated 40V dc power supplies. For firing of each IGBT switch, a Gate driver board is designed utilizing EXB840 Fuji IGBT-driving IC and TLP521 photo-coupler for isolating the power circuit and the DSP board. In addition, a protection board is designed to amplify the current values of DSP ports using 74HCT244N Buffer IC. It also prevents simultaneous conduction of up and down switches using 74ALS08 NAND and 74HC4078 OR ICs by controlling the enable pin of the Buffer IC. The aforementioned PWM switching techniques are programmed with Code Composer Studio (CCS) and are implemented utilizing a TMS320F2812 Digital Signal Processor (DSP) board, which is connected to a PC through a XDS100 Emulator to compile and load the programs. An Instek GDS-820 digital oscilloscope has been utilized to monitor and capture the results. A photograph of the proposed CHB-VSI experimental setup is represented in Fig. 33.

In order to achieve similar voltage waveforms to Fig. 9 to Fig. 15, the amplitude modulation term m_a is considered equal to 0.9 and the frequency modulation term m_f is accommodated correspondingly. The obtained waveforms for different PWM switching techniques are represented in Fig. 34 to Fig. 40.

The hardware set-up parameters are as follows:

A resistive load R=1.1 KΩ; each dc sources V_{dc}=9 V; fundamental frequency f_1=50 Hz. The pulses are produced with an accuracy of 100 μs.

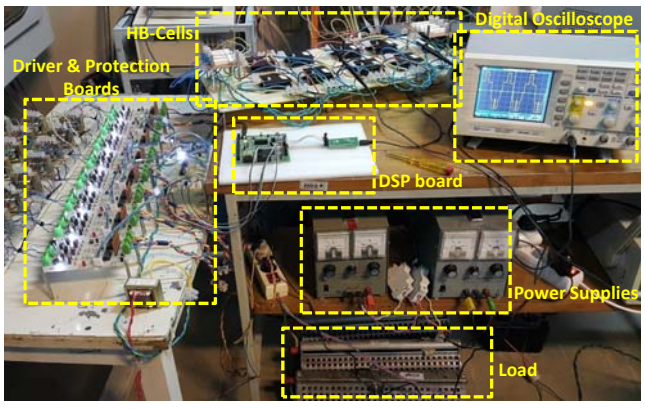

Figure 33. Photograph of CHB-VSI experimental setup

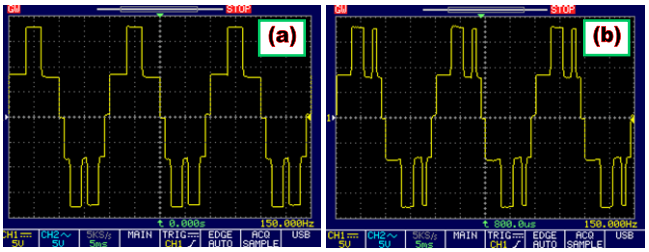

Figure 34. The CHB output voltage with PD-PWM for a) m_f=4, b) m_f=5

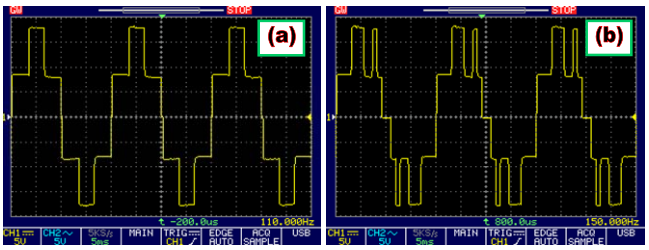

Figure 35. The CHB output voltage with POD-PWM for a) m_f=4, b) m_f=5

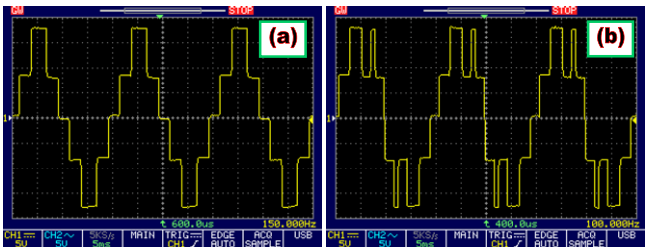

Figure 36. The CHB output voltage with APOD-PWM for a) m_f=4, b) m_f=5

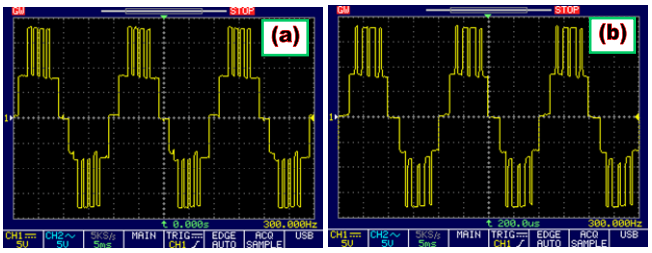

Figure 37. The CHB output voltage with PS-PWM for a) m_f=4, b) m_f=3

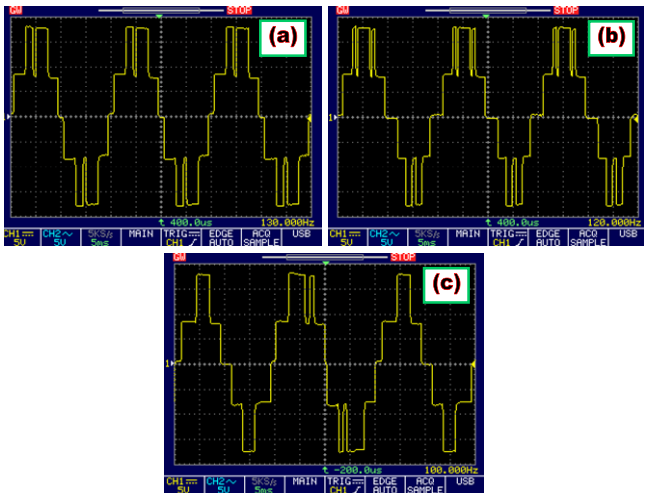

Figure 38. The CHB output voltage with R-APOD-PWM for a) m_f=4, b) m_f=6, c) m_f=3

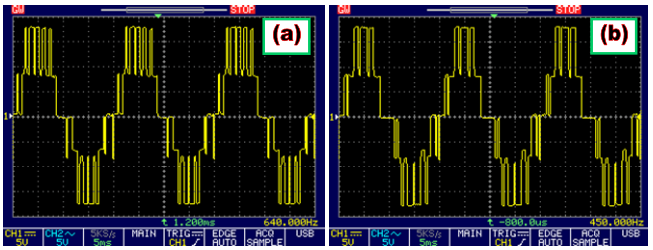

Figure 39. The CHB output voltage with H1-PWM for a) m_f=4, b) m_f=3

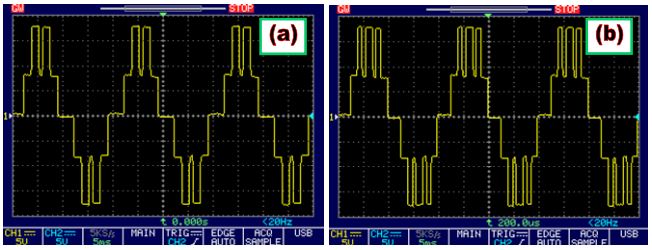

Figure 40. The CHB output voltage with H2-PWM for a) m_f=4, b) m_f=5

It can be clearly seen that the experimental results (Fig. 34 to Fig. 40) are similar to the simulation results (Fig. 9 to Fig. 15) which approves the accuracy of the simulation results.

VI. Conclusion

This paper has evaluated the effect of various multi-carrier based PWM techniques on harmonic distortion of the CHB multilevel inverter. For this purpose, the CHB output voltage and the input current at ac grid side have been investigated. In this work, different PWM switching methods such as PD-PWM, POD-PWM, APOD-PWM, PS-PWM, H1-PWM, H2-PWM, R-PD-PWM, R-POD-PWM and, R-APOD-PWM have been experimentally implemented. According to the results, among various PWM switching techniques, the R-LS-PWM (i.e. R-PD-PWM, R-POD-PWM, and R-APOD-PWM) methods reduce the harmonic content of input current while keeping the obvious advantage of LS-PWM methods that is lower phase and line-to-line voltages distortion. Specially, the proposed R-APOD-PWM switching strategy offers superior preferences including lower voltage distortion at odd frequency term (m_f) values.

Appendix A

Power grid parameters: V_{AB}=220 V, R_S=0.135 Ω, L_S=162.34 μH

dc-link capacitor: 400 mF

The Δ/Y transformer is composed of three single-phase transformers. Single-phase transformer parameters: N=220/220, L_m=1500 mH, R_m=1000 Ω, R_1=0.5 Ω, L_1=0.4 mH, R_2=0.5 Ω, L_2=0.4 mH

The Δ/Δ transformer is composed of three single-phase transformers. Single-phase transformer parameters: N=220/380, L_m=1500 mH, R_m=1000 Ω, R_1=0.5 Ω, L_1=0.4 mH, R_2=1.5 Ω, L_2=1.2 mH

The load parameters are as follows:

R-L load: R=2 Ω , L_1=1 mH.

R-C load: R=2 Ω, C=10.143 mF (considering $Z_{L1}=Z_C$, $\omega L_1=(\omega C)^{-1}$).

R-L-C load: R=2 Ω, L_2=100 μH, C=10.143 mF.

References

[1] J. Rodriguez, J. S. Lai, F. Z. Peng, "Multilevel inverters: A survey of topologies, controls, and applications," IEEE Transaction on Industrial Electronics, vol. 49, no. 4, pp. 724-738, Aug. 2002. doi: 0.1109/TIE.2002.801052

[2] J. Rodriguez, S. Bernet, B. Wu, J. O. Pontt, S. Kouro, "Multilevel voltage-source-converter topologies for industrial medium-voltage drives," IEEE Transaction on Industrial Electronics, vol. 54, no. 6, pp. 2930-2945, Dec. 2007. doi: 10.1109/TIE.2007.907044

[3] B. Wu, "High-Power Converters and AC Drives", pp. 119-141, Wiley-IEEE Press, 2006.

[4] D. G. Holmes, T. A. Lipo, "Pulse Width Modulation for Power Converters: Principles and Practice", pp. 433-528, Wiley-IEEE Press, 2003.

[5] Rodriguez, S. Bernet, B. Wu, J. O. Pontt, S. Kouro, "Comparison of neutral-point-clamped, symmetrical, and hybrid asymmetrical multilevel inverters voltage," IEEE Transaction on Industrial Electronics, vol. 57, no. 7, pp. 2297-2306, July 2010. doi: 10.1109/TIE.2010.2040561

[6] R. Teodorescu, F. Blaabjerg, J. K. Pedersen, E. Cengelci, P. N. Enjeti, "Multilevel inverter by cascading industrial VSI," IEEE Transaction on Industrial Electronics, vol. 49, no. 4, pp. 832-838, Aug. 2002. doi: 10.1109/TIE.2002.801069

[7] N. Karnik, D. Singla, P. R. Sharma, "Comparative analysis of harmonic reduction in multilevel inverter," The 5th IEEE Power India Conference, Murthal, India, Dec. 2012, pp. 1-5. doi: 10.1109/PowerI.2012.6479521

[8] A. Bendre, G. Venkataramanan, D. Rosene, V. Srinivasan, "Modeling and design of a neutral-point voltage regulator for a three-level diode-clamped inverter using multiple-carrier modulation," IEEE Transaction on Industrial Electronics, vol. 53, no. 3, pp. 718-726, Aug. 2002. doi: 10.1109/TIE.2006.874424

[9] B. P. McGrath, D. G. Holmes, "Multicarrier PWM strategies for multilevel inverters," IEEE Transaction on Industrial Electronics, vol. 49, no. 4, pp. 858-867, Aug. 2002. doi: 10.1109/TIE.2002.801073

[10] R. Naderi, A. Rahmati, "Phase-shifted carrier PWM technique for general cascaded inverters," IEEE Transaction on Power Electronics, vol. 23, no. 3, pp. 1257-1269, May. 2008. doi: 10.1109/TPEL.2008.921186

[11] G. Carrara, S. Gardella, M. Marchesoni, R. Salutari, G. Sciutto, "A new multilevel PWM method: a theoretical analysis," IEEE Transaction on Power Electronics, vol. 7, no. 3, pp. 497–505, July 1992. doi: 10.1109/63.145137

[12] L. M. Tolber, T. G. Habetler, "Novel multilevel inverter carrier based PWM method," IEEE Transaction on Industry Applications, vol. 35, no. 5, pp. 1098–1107, Oct. 1999. doi: 10.1109/28.793371

[13] M. Perez, S. Kouro, J. Rodriguez, B. Wu, "Modified staircase modulation with low input current distortion for multicell converters," IEEE Power Electronics Specialists Conference (PESC), Rhodes, Greece, June 2008, pp. 1989-1994. doi: 10.1109/PESC.2008.4592235

[14] C. Govindaraju, K. Baskaran, "Efficient sequential switching hybrid-modulation techniques for cascaded multilevel inverters," IEEE Transaction on Power Electronics, vol. 26, no. 6, pp. 1639-1648, June 2011. doi: 10.1109/TPEL.2010.2089064

[15] M. Angulo, P. Lezana, S. Kouro, J. Rodriguez, B. Wu, "Level-shifted PWM for cascaded multilevel inverters with even power distribution," The 38th Annual Power Electronics Specialists Conference (PESC'07), Orlando, Florida, USA, June 2007, pp. 2373–2378. doi: 10.1109/PESC.2007.4342382

[16] P. Palanivel, S. S. Dash, "Analysis of THD and output voltage performance for cascaded multilevel inverter using carrier pulse width modulation techniques," IET Power Electronics, vol. 4, no. 8, pp. 951-958, 2011. doi: 10.1049/iet-pel.2010.0332

[17] D. Patel, R. Saravanakumar, K. K. Ray, R. Ramesh, "A review of various carrier based PWM methods for multilevel inverter," International Conference on Power Electronics (IICPE), India, Jan. 2011, pp. 1-6. doi: 10.1109/IICPE.2011.5728059

[18] M. Calais, L. J. Borle, V. G. Agelidis, "Analysis of multicarrier PWM methods for a single-phase five level inverter," The 32nd Power Electronics Specialists Conference (PESC), Vancouver, Canada , June 2001, vol. 3, pp. 1351-1356. doi: 10.1109/PESC.2001.954308

[19] T. Wang and Y. Zhu, "Analysis and comparison of multicarrier PWM schemes applied in H-bridge cascaded multi-level inverters," The 5th Conference on Industrial Electronics and Applications (ICIEA), Taichung, Taiwan, June 2010, pp. 1379-1383. doi: 10.1109/ICIEA.2010.5514885

[20] P. Hamedani, A. Shoulaie, "Indirect field oriented control of linear induction motors considering the end effects supplied from a cascaded H-bridge inverter with multiband hysteresis modulation," IEEE 2013 Power Electronics Drive Systems and Technologies Conference (PEDSTC), Tehran, Iran, Feb. 2013, pp. 13-19. doi: 10.1109/PEDSTC.2013.6506665